Time reversed imaging for perturbed media

Kurang Mehta and Roel Snieder
Center for Wave Phenomena, Department of Geophysics, Colorado School of Mines, Golden, Colorado 80401

(Received 23 November 2004; accepted 16 December 2005)

In time reversed imaging a pulse is propagated through a medium, the signal is recorded, and then the time reversed signal is back-propagated through the same medium to refocus the energy at the original location of the source. The refocusing is independent of the medium if the medium is the same during back-propagation. If the speed of back-propagation differs from the speed of forward propagation, the waves refocus at a different location. For a single source and single receiver, the shift is proportional to the distance between the source and the receiver and the speed difference. If several receivers are placed along a circle to form an aperture angle, the shift in the location of the refocused pulse increases with increasing aperture angle for a given source-receiver distance and speed difference. If we analyze the problem using ray theory, an increase in the aperture angle would result in a decrease in the shift of the refocused pulse. The explanation for the shift of the refocused pulse with aperture angle is simple from a wave-front point of view.
[DOI: 10.1119/1.2166365]

I. TIME REVERSED IMAGING

In time reversed imaging a pulse is propagated through a medium, the signal is recorded, and then the time reversed signal is back-propagated through the same medium to refocus the energy at the original source location. The refocusing takes place in time and space and occurs in homogeneous as well as heterogeneous media. The refocused pulse is independent of the characteristics of the medium if the same medium is used for the forward- and the back-propagation.[1] A heterogeneous medium enhances the degree of refocusing.[2] Back-propagation is equivalent to a convolution of the time reversed signal with the impulse response of the medium. The only difference between the theoretical expressions for convolution and correlation is that in the latter both functions have the same sign for the time variable, and in convolution the time of one of the functions is reversed. Hence, back-propagation is equivalent to the correlation of the recorded signal and the impulse response of the medium. Parvulescu[3] has shown that this similarity between convolution and correlation can be be exploited by using a matched filter[4,5] in which the medium's impulse response is the time reverse of one of the correlands.

Time reversed imaging has been applied in several areas of science and engineering. For example, the technique has been used as a noninvasive method to refocus energy on kidney stones. The kidney stone receives a signal and scatters it in all directions. A mirror array picks up the scattered signal, amplifies it, and sends the signal back to refocus the energy at the source of the scattered waves, that is, the kidney stone. Another medical application of time reversed imaging is acoustically induced hyperthermia for tumor treatment.[6] Time reversed imaging is also used to detect defects in metals, to detect mines in the ocean,[7] and for secure communication.[3,8–10]

The back-propagation of a signal is mathematically the same as the process of migration in geophysics.[11] In a standard geophysical experiment, sources are placed on the earth's surface. These sources generate waves that physically propagate into the subsurface. The subsurface (earth's interior) is heterogeneous in terms of the velocity of propagation of the waves. Because of the velocity contrast, some of the waves are reflected back to the surface. These reflected waves are recorded using receivers on the surface. These recorded waves comprise the data for geophysicists, and this data acquisition process represents the forward-propagation, input to time reversed imaging. In time reversed imaging the signal recorded at the receiver array is back-propagated physically through the same medium to refocus energy at the source location. An analogy between geophysical migration and time reversed imaging can be stated as follows. The waves reflected from the subsurface are recorded on the surface and migrated (mathematically same as back-propagated) using an estimate of the velocity of the subsurface (also called the estimated velocity model). An estimated velocity model is used because in the process of migration, we do not back-propagate the recorded signal physically into the subsurface. Rather, the recorded wave-field is migrated using computer simulation, thus helping us estimate the image of the earth's subsurface. Because the estimated velocity model does not include the precise variations in the actual velocity structure of the earth's subsurface (also called the true velocity model), if we migrate the recorded wave-field with this estimate of the velocity model, the resulting image will be inaccurate. These inaccuracies translate into discrepancies in the locations where the waves focus. The discrepancy in the focusing depends on the difference between the true and the estimated velocity models. A process called *migration velocity analysis*[12] is used to iterate toward the best estimate of the velocity model by minimizing the focusing discrepancies.

When the same medium is used for forward- and backward-propagation, the refocusing of the energy occurs at the location of the original source. However, when the back-propagation speed differs from the forward-propagation speed, the waves refocus at other locations. The difference in the forward and backward speeds can be determined from the shift of the refocused pulse compared to the original source location.

In coda wave interferometry a single source and a receiver are used to study velocity differences.[13,14] The changes are monitored by the correlation of the coda waves recorded in the unperturbed and perturbed medium, respectively. This

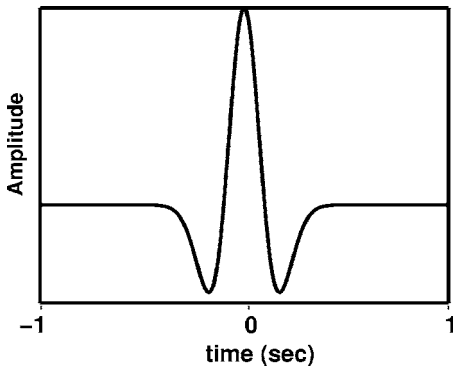

Fig. 1. The shape of the Ricker wavelet with $\alpha=10$.

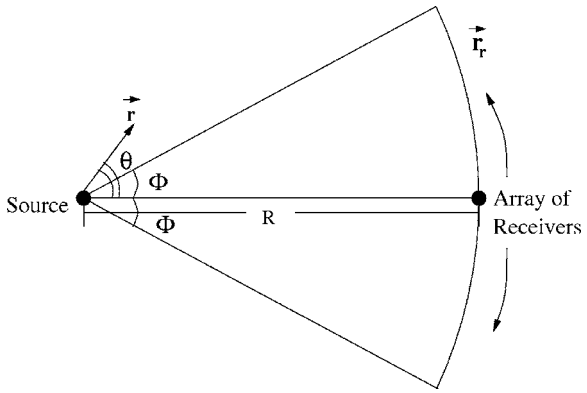

Fig. 2. The source and an array of receivers placed at a distance R for an aperture angle Φ.

technique is based on the high sensitivity of multiple scattered waves to small changes in a medium and can be used to monitor changes in volcanic interiors.[15,16] For a single receiver, time reversed imaging at the source location is the same as convolution with the time-reversed signal, which is the same as correlation with the originally recorded signal. The shift in the location of the refocused pulse for a perturbed medium is related to the deviation of the correlation peak from the origin, which gives a measure of the velocity change. Hence for a single source and receiver, time reversed imaging is identical to coda wave interferometry.

If we have an array of receivers, the shift in the location of the refocused pulse depends on the aperture angle, the distance between the source and receiver, and the velocity change. In Sec. II we derive the shift in the location of the refocused pulse, followed by a simulation to validate the result.

II. LOCATION OF THE REFOCUSED PULSE

We start with a simple model to study the effect of a velocity change on the location of the refocused pulse. The model is acoustic, two-dimensional, and homogeneous. We allow a source pulse to propagate through the homogeneous medium using the 2D wave equation and record the field at a distance R with an array of receivers. The wave-field recorded at the receivers is then time reversed and back-propagated through the same medium to refocus the energy at the source location.

Let the source be a symmetric pulse such as a Ricker wavelet $S(t)$ given by[17]

$$S(t)=\frac{\partial^2}{\partial t^2}[\exp(-\alpha^2t^2/2)]. \tag{1}$$

Figure 1 shows the shape of the Ricker wavelet. The Ricker wavelet is zero-phase in the language of geophysics and signal processing. We propagate this pulse over a distance R and record the wave-field at a circular array of receivers. The receivers are placed along a circle of radius R with the source at the center and a fixed aperture angle $\pm\Phi$ as shown in Fig. 2. The far wave-field can be represented in the frequency domain as a product of the source term and the solution to the Helmholtz equation in polar coordinates using the 2D asymptotic behavior of the Hankel function:[18–20]

$$u(\omega,R)=\frac{\exp[i(kR-\pi/4)]}{\sqrt{8\pi kR}}S(\omega), \tag{2}$$

where k is the wavenumber. This form of u is the same as the convolution of the time-domain source wavelet with an impulse response. When this wave-field is reversed in time, it acts as a new source signal.

The reversal of time in the time domain is equivalent to complex conjugation in the frequency domain. If $S(t)$ is the time-dependent part of the wave-field, it can be represented in the frequency domain using the Fourier transform,

$$S(\omega)=\int_{-\infty}^{\infty}S(t)e^{i\omega t}\,dt \Leftrightarrow S(t)=\frac{1}{2\pi}\int_{-\infty}^{\infty}S(\omega)e^{-i\omega t}\,d\omega. \tag{3}$$

The time reversed wave-field is

$$S(-t)=\frac{1}{2\pi}\int_{-\infty}^{\infty}S(\omega)e^{+i\omega t}\,d\omega=\frac{1}{2\pi}\int_{-\infty}^{\infty}S(-\omega)e^{-i\omega t}\,d\omega. \tag{4}$$

For a real signal, $S(-\omega)$ equals the complex conjugate $S^*(\omega)$,

$$S(-t)=\frac{1}{2\pi}\int_{-\infty}^{\infty}S^*(\omega)e^{-i\omega t}\,d\omega. \tag{5}$$

Equation (5) shows that the time reversed signal in the time domain is equivalent to complex conjugation in the frequency domain. Hence, the wave-field recorded by the array of receivers shown in Fig. 2 is equivalent to complex conjugation of Eq. (2) when reversed in time:

$$u^*(\omega,R)=\frac{\exp[-i(kR-\pi/4)]}{\sqrt{8\pi kR}}S^*(\omega). \tag{6}$$

If we back-propagate this wave-field with the same speed as the forward propagating speed, we refocus the waves at the original source location. When we back-propagate with a different speed, the energy will refocus at a location other than at the original source. Let us see what information this shift in the location of the refocused pulse gives about the change in the speed. The back-propagated wave-field radiated by each of the receivers is obtained by the convolution of the time reversed signal with the impulse response (also known as the Green's function[18,20]). This convolution gives the back-propagated wave-field recorded at the source location due to each receiver. To calculate the total back-

propagated wave-field, we need to sum over all receivers that have recorded the forward-propagating wave. If we assume that the receivers in the receiver array are closely spaced, we may approximate the sum all the receivers by integration over the aperture angle Φ. Hence, in the frequency domain the back-propagated wave-field at location $\mathbf{r}$ corresponds to

$$P(\mathbf{r},\omega)=\int_{-\Phi}^{\Phi} G[\mathbf{r},\mathbf{r}_r(\phi)]u^*(\omega,R)d\phi \tag{7a}$$

$$=S^*(\omega)\int_{-\Phi}^{\Phi}\frac{\exp[i(k'|\mathbf{r}-\mathbf{r}_r|-\pi/4-kR+\pi/4)]}{\sqrt{8\pi k'|\mathbf{r}-\mathbf{r}_r|}\sqrt{8\pi kR}}\,d\phi, \tag{7b}$$

where $\mathbf{r}_r$ is the receiver location and k and k' are the wavenumbers associated with forward- and back-propagation, respectively.

We are interested in the refocusing point close to the original source location. Further analysis near the refocusing point requires that $R\gg r$ and hence the term $|\mathbf{r}-\mathbf{r}_r|$ in Eq. (7b) can be approximated to second-order accuracy in r/R as

$$|\mathbf{r}-\mathbf{r}_r|=R\left[1-\left(\frac{r}{R}\right)\cos(\theta-\phi)+\left(\frac{r^2}{2R^2}\right)\sin^2(\theta-\phi)\right], \tag{8}$$

where the angle θ is defined in Fig. 2. We ignore the dependence of $|\mathbf{r}-\mathbf{r}_r|$ on r/R in the denominator of Eq. (7b) and approximate it by R. This approximation results in an error of order r/R, which can be ignored because $R\gg r$. In the numerator, the term $|\mathbf{r}-\mathbf{r}_r|$ is multiplied by the wavenumber k in the argument of an exponent. If we ignore the (r/R) and $(r/R)^2$ terms in the numerator of Eq. (7), the errors would be the order of (r/λ) and $(r^2/\lambda R)$, respectively, which may be significant, where λ is the wavelength of the pulse. We therefore express $|\mathbf{r}-\mathbf{r}_r|$ in the exponent of Eq. (7b) using Eq. (8). With this simplification, the denominator becomes a constant scaling factor except for $|\omega|$ which comes from the product of the terms $\sqrt{k}$ and $\sqrt{k'}$ in the denominator. If we omit this scaling factor, the back-propagated wave-field becomes the following integral over all the receivers:

$$P(\mathbf{r},\omega)=\frac{S^*(\omega)}{|\omega|}\int_{-\Phi}^{\Phi}\exp\left[-i\left\{k'r\cos(\theta-\phi)-\frac{1}{2}\left(\frac{k'r^2}{R}\right)\sin^2(\theta-\phi)-R(k'-k)\right\}\right]d\phi. \tag{9}$$

We let $k=\omega/c$ and $k'=\omega/c'$ and rewrite the back-propagated wave-field as

$$P(\mathbf{r},\omega)=\frac{S^*(\omega)}{|\omega|}\int_{-\Phi}^{\Phi}\exp\left\{-i\omega\left[\left(\frac{r}{c'}\right)\cos(\theta-\phi)-\frac{1}{2}\left(\frac{r^2}{Rc'}\right)\sin^2(\theta-\phi)-R\left(\frac{1}{c'}-\frac{1}{c}\right)\right]\right\}d\phi, \tag{10}$$

where c is the forward-propagation speed of the and c' is the back-propagation speed.

To represent the refocused energy in the time domain we integrate over all frequencies.[21] The wave-field can be represented in the time domain in terms of the function f as

$$P(\mathbf{r},t)=\int_{-\Phi}^{\Phi} f\left[t+\left(\frac{r}{c'}\right)\cos(\theta-\phi)-\frac{1}{2}\left(\frac{r^2}{Rc'}\right)\sin^2(\theta-\phi)-R\left(\frac{1}{c'}-\frac{1}{c}\right)\right]d\phi, \tag{11}$$

where f is defined as

$$f(t)=\int_{-\infty}^{\infty}\frac{S^*(\omega)}{|\omega|}e^{-i\omega t}\,d\omega. \tag{12}$$

The function f is a function of time and space and can be expressed in terms of x and z as

$$\begin{aligned} &f\left[t+\left(\frac{r}{c'}\right)\cos(\theta-\phi)-\frac{1}{2}\left(\frac{r^2}{Rc'}\right)\sin^2(\theta-\phi)-R\left(\frac{1}{c'}-\frac{1}{c}\right)\right]\\ &=f\left[t+\left(\frac{z}{c'}\right)\cos\phi+\left(\frac{x}{c'}\right)\sin\phi-\left(\frac{1}{2c'R}\right)(x\cos\phi-z\sin\phi)^2-R\left(\frac{-\delta c}{cc'}\right)\right], \end{aligned} \tag{13}$$

where

$$z=r\cos\theta, \tag{14a}$$

$$x=r\sin\theta, \tag{14b}$$

$$\delta c\equiv c'-c. \tag{14c}$$

The function f can be approximated using a Taylor's series expansion to second order in ξ, where

$$\xi=\left(\frac{z}{c'}\right)\cos\phi+\left(\frac{x}{c'}\right)\sin\phi-\left(\frac{1}{2c'R}\right)(x\cos\phi-z\sin\phi)^2-R\left(\frac{-\delta c}{cc'}\right). \tag{15}$$

If we insert this representation into Eq. (11) and integrate over ϕ, we obtain an expression for the back-propagated wave-field at an arbitrary location (x,z) close to the source location.

We are interested in the location of the refocused pulse, which we define as the maximum value of this wave-field at time $t=0$. Because the medium is homogeneous and the acquisition geometry is symmetric with respect to $x=0$, the peak is located on the x-axis; hence we set $x=0$ in the wave-field representation. The resultant wave-field representation involves terms in z and t only. The shift in the location of the refocused pulse in the z-direction can be calculated in two steps. The first step involves evaluating the wave-field at $t=0$. This wave-field is then solved for its maximum as a function of z. The resultant shift in the location of the refocused pulse is

$$\delta z\cong\frac{-2((\sin\Phi)/\Phi)R(\delta c/c)}{1+(\sin 2\Phi)/2\Phi}. \tag{16}$$

A derivation of this result is given in the Appendix.

Equation (16) for the shift in the location of the refocused pulse holds for any source pulse that is symmetric at $t=0$ (as shown in Fig. 1). When the forward- and backward-

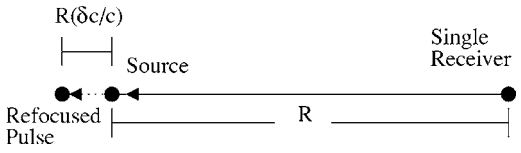

Fig. 3. The shift in the location of the refocused pulse when the wave-field is recorded by a single receiver and back-propagated with a higher velocity (based on ray theory).

propagating velocities are the same ($\delta c=0$), the location of the refocused pulse is the same as that of the source pulse ($\delta z=0$), as shown in Eq. (16). For a small aperture angle, $\sin\Phi/\Phi$ and $\sin 2\Phi/2\Phi \rightarrow 1$; hence $\Phi \rightarrow 0$, and the shift of the refocused pulse is a function of just the distance R and the velocity change δc:

$$\lim_{\Phi\rightarrow 0} \delta z = -R\left(\frac{\delta c}{c}\right). \tag{17}$$

Let us consider the case of small Φ or equivalently only a single receiver (see Fig. 3). Suppose we excite the source pulse and record the signal at a distance R using a single receiver. If this recorded signal is back-propagated with the same speed, then the back-propagated wave-field refocuses at the original source location. If, instead, the back-propagation speed is different from the forward-propagation speed ($\delta c \neq 0$), the back-propagated waves travel over a distance,

$$R_{\text{back}} = c't = (c+\delta c)t = ct + t\delta c = R - \left[-R\left(\frac{\delta c}{c}\right)\right]. \tag{18}$$

Hence, the relative shift in the location of the refocused pulse is $-R(\delta c/c)$, which agrees with Eq. (17), suggesting that our expression in Eq. (16) also holds for aperture angles of 0°, that is, just a single receiver.

III. ILLUSTRATION USING NUMERICAL SIMULATION

Equation (16) gives the location of the refocused pulse. Let us compare the results obtained from this expression with a simulation. The simulation uses a finite-difference scheme for the 2D wave equation with absorbing boundary conditions.[22] The geometry of the simulation is shown in Fig. 4. Because the medium is homogeneous, we specify a constant speed for forward propagation. The source radiation pattern is isotropic as illustrated by the arrows. The receiver array at the distance $R=20\lambda$, where λ is the wavelength of the pulse, records the wave field. The aperture angle $\Phi=35°$ for this example. When this wave-field is time-reversed and back-propagated using the same speed as for forward propagation, the waves refocus at the original source location as shown in Fig. 5. We also see some low amplitude numerical noise near the sides, which is caused by reflection from the imperfectly absorbing boundaries.

Even though its location is preserved, the shape of the refocused pulse differs from that of the original pulse in Fig. 4. One reason for this distortion is that the receiver array has a finite aperture $\Phi=35°$. During forward propagation, the source propagates in all possible directions, while in back-propagation the energy propagates only from a certain slice of directions. In addition, according to Eq. (9), the refocused pulse is proportional to $S^*(\omega)/|\omega|$ for a given source spectrum $S(\omega)$. This distortion can be seen more clearly in Fig. 6 which is a detailed view of Fig. 5.

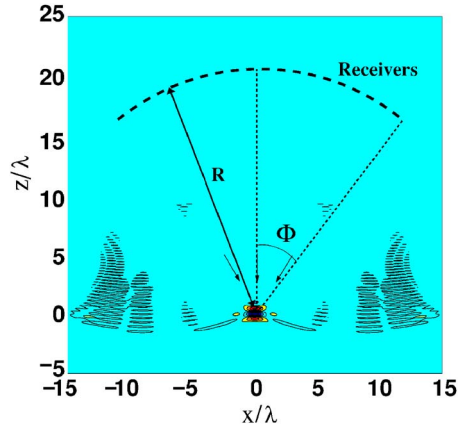

Fig. 5. Energy refocusing at the source location (along with some low amplitude noise caused by imperfect absorbing boundary conditions) obtained after the wave-field recorded by the receivers is back-propagated using the correct back-propagating velocity.

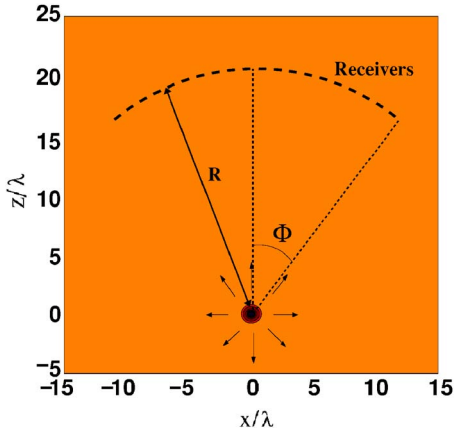

Fig. 4. Initial conditions of the simulation showing a source pulse at the origin with an array of receivers forming an aperture angle Φ at a distance R.

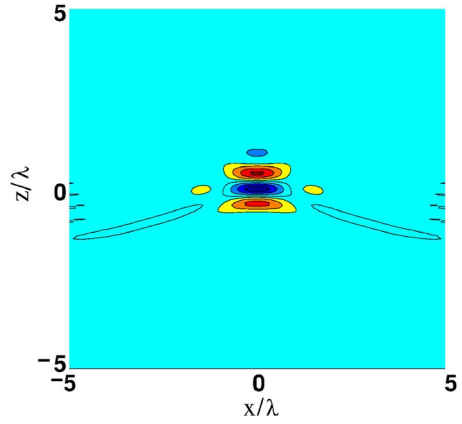

Fig. 6. A detailed view of the refocused pulse obtained by back-propagating the wave-field using the correct velocity. Even though the pulse is focused at the correct location, there is distortion in the shape of the refocused pulse.

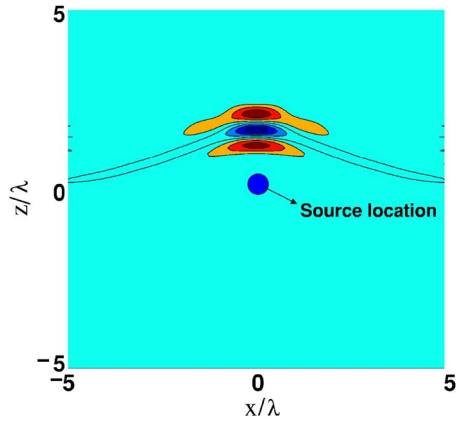

Fig. 7. The refocused pulse obtained when the recorded wave-field is back-propagated using a lower velocity than for forward-propagation.

Let us see what happens when we back-propagate with a different speed. Suppose the back-propagating speed c' is small compared to the speed c for the forward propagation. When the back-propagating speed is lower than the forward-propagating speed, the refocusing occurs at a location closer to the receiver array compared to the original source location, which is indicated by a circle in Fig. 7. Because the shape of the refocused pulse is similar to a frown, this shape is commonly referred to as a frown in seismic migration.[12] Figure 8 shows the refocused pulse when the back-propagating speed is higher than the speed of forward-propagation. The refocusing in this case occurs at a location farther from the receiver array and the shape of the refocused pulse resembles a smile.[12]

Table I shows the agreement between the shift in the location of the refocused pulse obtained from Eq. (16) and the simulation for various velocity changes at the aperture angle of 35°. This result holds for any aperture angle ranging from as small as 5°, which mimics the case of a single receiver, up to 90°. Apart from the distortion in the shape of the refocused pulse, the shift in its location obtained from the simulation agrees with Eq. (16).

The change in the location of the refocused pulse with a change in the velocity for two extreme cases ($\Phi=5°$ and 90°) is demonstrated in Fig. 9. The solid line shows the shift in the location of the refocused pulse as given by Eq. (16) and the points show the shift obtained from the simulations. The latter agree with Eq. (16) for small velocity differences with an accuracy of $|0.044-0.042|/|0.042|=5\%$. As we increase the velocity difference for larger aperture angles, Eq. (16) becomes less accurate and begins to deviate from the simulation results. As we increase the velocity difference, the second-order approximation in ξ [Eq. (15)] used in the Taylor's expansion of the function f and the expansion of $|\mathbf{r}-\mathbf{r}_r|$ in Eq. (8) become inaccurate, thus leading to the deviation.

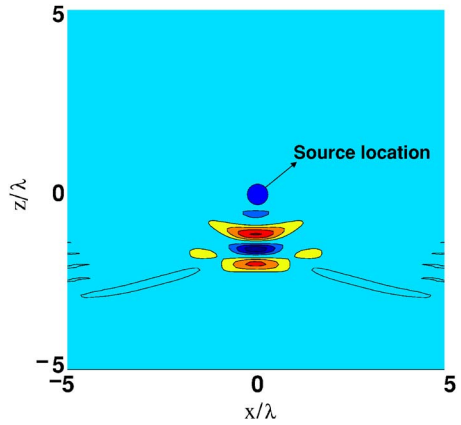

Fig. 8. The refocused pulse obtained when the recorded wave-field is back-propagated using a higher velocity than for forward-propagation.

Table I. Comparison of theoretical and numerical results showing the relative shift in the location of the refocused pulse for different relative velocity changes. The aperture angle is 35°.

$\delta c/c$	$-\delta z/R$ (theoretical)	$-\delta z/R$ (numerical)
−0.04	−0.042	−0.044
−0.02	−0.021	−0.021
0.00	0	0
0.02	0.021	0.021
0.04	0.042	0.044

IV. WHY DO RAYS MISGUIDE US?

In high-quality migration velocity analysis, the 5% accuracy of Eq. (16) discussed in Sec. III is typical and becomes worse as we consider more complex media. Equation (16) is accurate (up to 5%) under certain conditions which include a bound on the relative velocity difference of $\approx\pm5\%$. The accuracy also depends on the normalized distance (R/λ) between the source and the receivers and, more importantly, the aperture angle Φ. The angle Φ is a crucial parameter in determining the shift in the location of the refocused pulse.

We start by analyzing the influence of the aperture angle on the refocused pulse in terms of ray theory. Consider a very small aperture or equivalently a single receiver. Equation (17) shows that for a very small aperture angle, the velocity change for back-propagation results in a relative shift in the location of the refocused pulse of $R(\delta c/c)$. Figure 3 gives a representation of this case. If we back-propagate with speed $c'>c$, the shift in the location of the refocused pulse depends on the product of the distance R and the difference δc as shown in the derivation of Eq. (18).

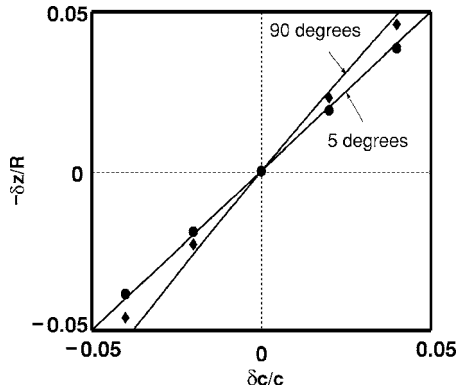

Fig. 9. The relative shift in the location of the refocused pulse as a function of the relative change in the back-propagating velocity. The relative shift obtained from the simulation is denoted by diamonds for $\Phi=90°$ and by circles for $\Phi=5°$.

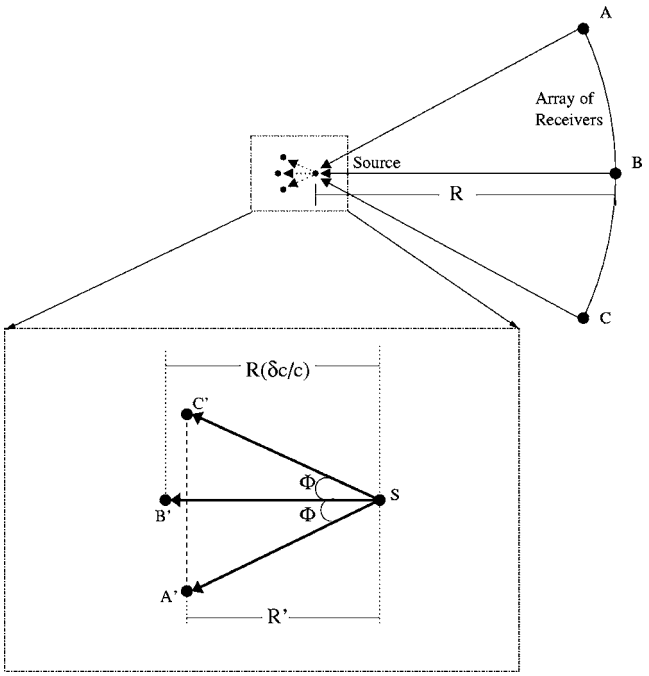

Fig. 10. The shift in the location of the refocused pulse when the wave-field is recorded by an array of receivers and back-propagated using a higher velocity (based on ray theory).

A more complicated case involves an array of receivers that form a finite aperture angle instead of a single receiver (see Fig. 10). We have seen that if we have only one receiver B, then the shift in the location of the refocused pulse is $R(\delta c/c)$ indicated by B′. Let us start by examining the contribution of the receivers A and C at the two ends of the receiver array. The rays coming from A and C also travel a distance of $R(\delta c/c)$, indicated by A′ and C′, respectively. The detailed view (in Fig. 10) shows the source S and the shift in the location of the refocused pulse for the three receivers A, B, and C. This shift is shown by the three rays in thick arrows each having the same length $R(\delta c/c)$. Even though the rays have the same length, the component of the rays $S-A'$ and $S-C'$ in the direction of $S-B'$ extends only up to a distance $R'=R(\delta c/c)\cos(\Phi)<R(\delta c/c)$, suggesting that for only two receivers at the two ends of the receiver array, the shift in the location of the refocused pulse is smaller than that of a single receiver.

Suppose that for a finite aperture angle several receivers are placed between A and C along the circular boundary. Rays coming from all the receivers travel a distance of $R(\delta c/c)$, but the contribution to the shift in the direction of $S-B'$ from each of the receivers is $R(\delta c/c)\cos\phi$, where the angle ϕ depends on the receiver location. This distance is always less than $R(\delta c/c)$. Hence, ray theory suggests that as we increase the aperture angle formed by the array of receivers, the shift in the location of the refocused pulse decreases.

Let us see if our results agree with this explanation. The slope of the two lines in Fig. 9 represents the ratio $(-\delta z)/[R(\delta c/c)]$. According to the ray theory explanation, the shift in the location of the refocused pulse decreases as we increase the aperture angle; hence, the slope of the line should decrease. Instead, the slope in Fig. 9 increases with increasing aperture angles ($\Phi=90°$).

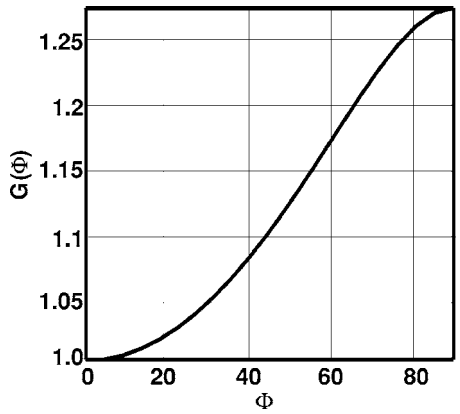

Fig. 11. The relative shift in the location of the refocused pulse normalized by the relative velocity change as a function of the angle Φ.

Let us consider the expression for the position of the refocused pulse, Eq. (16), which can be rewritten as

$$G(\Phi)\equiv\frac{-\delta z}{R(\delta c/c)}=2\frac{(\sin\Phi)/\Phi}{1+(\sin 2\Phi)/2\Phi}. \tag{19}$$

$G(\Phi)=1$ for $\Phi=0$. Figure 11 shows the plot of $G(\Phi)$ as a function of Φ. It shows that $G(\Phi)=1$ for $\Phi=0$ and it increases with increase in Φ, indicating that as Φ increases, the distance of the refocused pulse from the original pulse increases. This observation is supported in Fig. 9 which also shows an increase in the slope (of the line connecting the observation points) with an increase in Φ from 5° to 90°. This increase is contradicted by the reasoning based on the ray theory.

We now consider the explanation in terms of wave-front propagation. For the single receiver (see Fig. 12), the explanation remains the same as the ray theory and hence the shift in the location of the refocused pulse is $R(\delta c/c)$. The scenario is different when we consider more receivers and a larger aperture as shown in Fig. 13. Again consider just two receivers A and C placed at the ends. The detailed view in Fig. 13 shows the wave-fronts coming from receivers A, B, and C. The source is indicated by S and the dotted wavefronts indicate no velocity difference. The solid wave-fronts $A'-A''$, $B'-B''$, and $C'-C''$ are the three wavefronts from

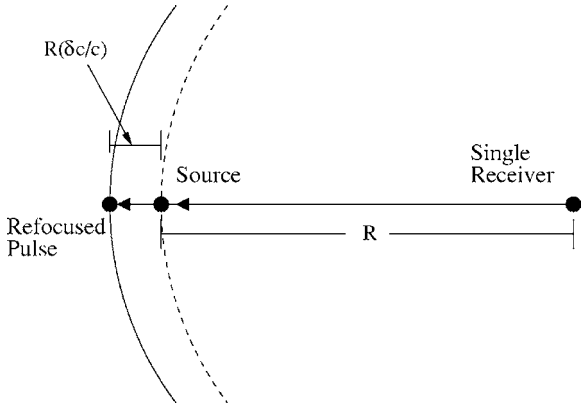

Fig. 12. The shift in the location of the refocused pulse when the wave-field is recorded by a single receiver and back-propagated using a higher velocity (based on wave theory).

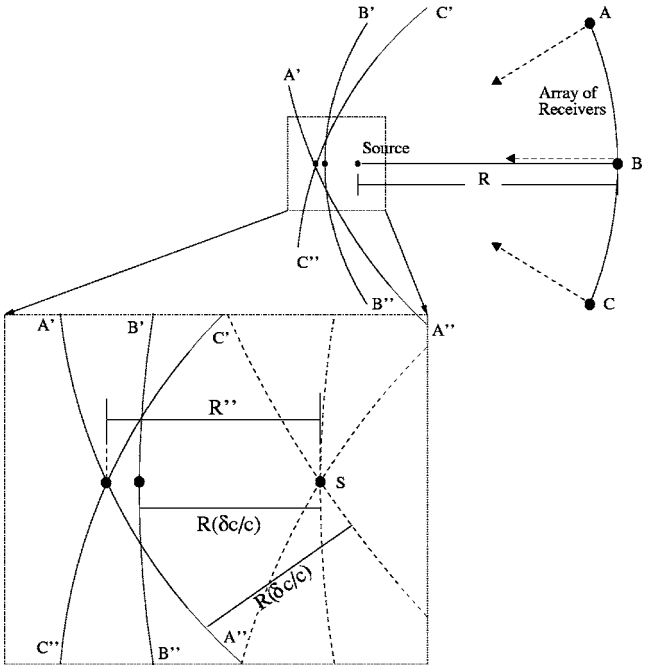

Fig. 13. The shift in the location of the refocused pulse when the wave-field is recorded by an array of receivers and back-propagated using a higher velocity (based on wave theory).

A, B, and C, respectively. All three wave-fronts are displaced by a distance of $R(\delta c/c)$ in their respective directions of propagation. It is the interference of the three wave-fronts that contributes to the refocused pulse. The wavefront propagating from the receiver A, $A'-A''$, has a displacement in the direction of $B'-B''$ given by $R''=[R(\delta c/c)/\cos(\Phi)] > R(\delta c/c)$. A similar explanation holds for the wave-front $C'-C''$; hence we have constructive interference at a distance R'' from the source, yielding the refocusing. The distance R'' is an apparent displacement. Hence for a larger aperture, the refocused pulse is shifted by a distance greater than $R(\delta c/c)$. This explanation is consistent with Eqs. (16) and (17) and supports the results shown in Figs. 9 and 11. When we consider the entire receiver array, the wave-fronts coming from all the receivers will be displaced by a distance of $R(\delta c/c)$ in their direction of propagation resulting in constructive interference at an effective distance $[R(\delta c/c)/\cos\Phi]$, with the angle Φ varying with the aperture of the receiver array. This distance may be less than or equal to R'', but will definitely be greater than $R(\delta c/c)$. Thus, if we consider the wave-fronts coming from the entire receiver array, the shift in the location of the refocused pulse will increase with increasing aperture angle. Hence, the results obtained from the theory and numerical simulation agree with the explanation based on wave-front propagation.

V. CONCLUSION

The principle idea of time reversed imaging is the refocusing of the energy at the same location as the source when the forwards- and back-propagating media are the same. Based on this idea, we have obtained an expression for the shift in the location of the refocused pulse caused by a velocity change during back-propagation. The shift depends mainly on the distance between the source and the receivers, the aperture angle formed by the receiver array, and the velocity change. For a single source-receiver pair, the shift is proportional to the velocity change and the source-receiver separation only. For more receivers the aperture angle plays an important role in determining the shift in the location of the refocused pulse. As we increase the aperture angle for the same source-receiver distance and velocity change, the shift in the location of the refocused pulse increases. An explanation based on the ray theory yields an underestimate of the shift because it is limited to approximating the wave-field with a few ray paths and this approximation does not completely take into account the effect of constructive interference of the wave-fronts giving the refocused pulse. The variation in the shift of the refocused pulse with a change in aperture angle is explained in terms of the constructive interference of wavefronts, which does include all the ray paths.

ACKNOWLEDGMENTS

We thank the support provided by the sponsors of the Consortium Project on Seismic Inverse Methods for Complex Structures at the Center for Wave Phenomena. We also appreciate the comments by and discussions with Dr. Ken Larner, Matt Haney, and Ivan Vasconcelos.

APPENDIX: DERIVATION OF THE SHIFT IN THE LOCATION OF THE REFOCUSED PULSE

The wave-field in the time domain is given by Eq. (11). When the function f is represented by a second-order Taylor series in r/R and integrated over all the receivers, we obtain the following expression for the back-propagated wave-field:

$$P(\mathbf{r},t) = 2\Phi f(t) + \dot{f}(t)I_1 + \tfrac{1}{2}\ddot{f}(t)I_2, \tag{A1}$$

where I_1 and I_2 are functions of $\mathbf{r}$. We need to calculate this wave-field at time $t=0$. We know that because of the symmetry of the receiver positions with respect to $x=0$, the peak location will occur at $x=0$. Hence, we can set $x=0$ in Eq. (A1). The integrals I_1 and I_2 are given by

$$\begin{aligned} I_1 &= \int_{-\Phi}^{\Phi}\left[\left(\frac{z}{c'}\right)\cos\phi - \left(\frac{z^2}{2c'R}\right)\sin^2\phi + R\left(\frac{\delta c}{cc'}\right)\right]d\phi \\ &= \left(\frac{2z}{c'}\right)\sin\Phi + 2R\Phi\left(\frac{\delta c}{cc'}\right) \\ &\quad - \left(\frac{z^2}{2Rc'}\right)\left[\Phi + \left(\frac{\sin 2\Phi}{2}\right)\right], \end{aligned} \tag{A2}$$

$$\begin{aligned} I_2 &= \int_{-\Phi}^{\Phi}\left[\left(\frac{z}{c'}\right)\cos\phi - \left(\frac{z^2}{2c'R}\right)\sin^2\phi + R\left(\frac{\delta c}{cc'}\right)\right]^2 d\phi \\ &= \left(\frac{z^2}{c'^2}\right)\left\{\Phi + \left(\frac{\sin 2\Phi}{2}\right) - \left(\frac{\delta c}{c}\right)\left[\Phi - \left(\frac{\sin 2\Phi}{2}\right)\right]\right\} \\ &\quad + 4R\left(\frac{\delta c}{cc'}\right)\left(\frac{z}{c'}\right)\sin\Phi - 2\Phi R^2\left(\frac{\delta c}{cc'}\right)^2. \end{aligned} \tag{A3}$$

In I_2 we consider only terms up to second order in z. If we insert these expressions for I_1 and I_2 in Eq. (A1) and set $t=0$, we obtain the wave-field as a quadratic function of z:

$$P(z,t) = A + Bz + Dz^2, \tag{A4}$$

where

$$A = \Phi\left[2f(0) + 2R\dot{f}(0)\left(\frac{\delta c}{cc'}\right) - R^2\ddot{f}(0)\left(\frac{\delta c}{cc'}\right)^2\right], \quad \text{(A5a)}$$

$$B = \left(\frac{2\sin\Phi}{c'}\right)\left[\dot{f}(0) + \ddot{f}(0)R\left(\frac{\delta c}{cc'}\right)\right], \quad \text{(A5b)}$$

$$D = \dot{f}(0)\left\{\frac{-\Phi}{2Rc'}\left[1 - \left(\frac{\sin 2\Phi}{2\Phi}\right)\right]\right\} + \ddot{f}(0)\left[\left(\frac{\Phi}{2c'^2}\right)K_1\right], \quad \text{(A5c)}$$

and

$$K_1 = 1 + \left[\frac{\sin 2\Phi}{2\Phi}\right] - \left(\frac{\delta c}{c}\right)\left[1 - \frac{\sin 2\Phi}{2\Phi}\right]. \quad \text{(A6)}$$

Because the source pulse is symmetric with respect to the origin, its first derivative vanishes at time $t=0$; hence $\dot{f}(0)=0$. The maximum value of the wave-field $P(z,t)$ at $t=0$ can be found by equating its first z-derivative to zero. The solution for z gives the shift in the location of the refocused pulse. This shift is $\delta z=-B/2D$ where the values of B and D at $t=0$ are given by

$$B = \ddot{f}(0)\left[\frac{2\sin\Phi}{c'}\right]R\left(\frac{\delta c}{cc'}\right), \quad \text{(A7)}$$

$$D = \ddot{f}(0)\left[\left(\frac{\Phi}{2c'^2}\right)K_1\right]. \quad \text{(A8)}$$

The corresponding value of δz is

$$\delta z = \frac{-2((\sin\Phi)/\Phi)R(\delta c/c)}{(1 + (\sin 2\Phi)/2\Phi) - (\delta c/c)(1 - (\sin 2\Phi)/2\Phi)}. \quad \text{(A9)}$$

The term $\ddot{f}(0)$ drops out in the expression for δz, which indicates that the shift in the location of the refocused pulse is independent of frequency. For small values of $(\delta c/c)$, we can ignore the second term in the denominator and hence

$$\delta z \cong \frac{-2((\sin\Phi)/\Phi)R(\delta c/c)}{(1 + (\sin 2\Phi)/2\Phi)}. \quad \text{(A10)}$$

[1] M. A. Haider, K. J. Mehta, and J. P. Fouque, "Time-reversal simulations for detection in randomly layered media," Waves Random Media **14**, 185–198 (2004).

[2] M. Fink and C. Prada, "Acoustic time-reversal mirrors," Inverse Probl. **17**, R1–R38 (2001).

[3] A. Parvulescu, "Matched-signal ("MESS") processing by the ocean," J. Acoust. Soc. Am. **98**, 943–960 (1995).

[4] G. L. Turin, "An introduction to matched filters," IRE Trans. Inf. Theory **IT-6**, 311–329 (1960).

[5] J. H. Karl, *An Introduction to Digital Signal Processing* (Academic, San Diego, CA, 1989).

[6] M. Porter, P. Roux, H. Song, and W. Kuperman, "Tumor treatment by time reversal acoustics," IEEE Proc. ICASSP-99 VI-2107, Phoenix, AZ (1999).

[7] M. Fink, "Time reversed acoustics," Sci. Am. **281**(11), 91–97 (1999).

[8] G. F. Edelmann, W. S. Hodgkiss, S. Kim, W. A. Kuperman, H. C. Song, and T. Akal, "Underwater acoustic communication using time reversal," Oceans 2001, Hawaii (2001).

[9] H. C. Song, W. A. Kuperman, W. S. Hodgkiss, T. Akal, S. Kim, and G. Edelmann, "Recent results from ocean acoustic time reversal experiments," 6th European Conference on Underwater Acoustics, Gdanski, Poland (2002).

[10] S. Kim, W. A. Kuperman, W. S. Hodgkiss, H. C. Song, G. F. Edelmann, T. Akal, R. P. Millane, and D. Di Iorio, "A method for robust time-reversal focusing in a fluctuating ocean," Oceans 2001, Hawaii (2001).

[11] L. Borcea, G. Papanicolaou, and C. Tsogka, "Theory and applications of time reversal and interferometric imaging," Inverse Probl. **19**, S139–S164 (2003).

[12] J. Zhu, L. R. Lines, and S. H. Gray, "Smiles and frowns in migration/velocity analysis," Geophysics **63**, 1200–1209 (1998).

[13] R. Snieder, "Coda wave interferometry," *McGraw-Hill Yearbook of Science and Technology 2004* (McGraw-Hill, New York, 2004), pp. 54–56.

[14] R. Snieder, A. Grêt, H. Douma, and J. Scales, "Coda wave interferometry for estimating nonlinear behavior in seismic velocity," Science **295**, 2253–2255 (2002).

[15] R. Snieder and M. Hagerty, "Monitoring change in volcanic interiors using coda wave interferometry: Application to Arenal Volcano, Costa Rica," Geophys. Res. Lett. **31**, L09608-1–5 (2004).

[16] A. Grêt, R. Snieder, R. C. Aster, and P. R. Kyle, "Monitoring rapid temporal changes in a volcano with coda wave interferometry," Geophys. Res. Lett. **32**, L06304-1–4 (2005).

[17] ⟨members.ozemail.com.au/~robgc/ricker.htm⟩.

[18] R. K. Snieder, *A Guided Tour of Mathematical Methods for the Physical Sciences* (Cambridge U. P., Cambridge, 2004), 2nd ed.

[19] G. B. Arfken and H. J. Weber, *Mathematical Methods for Physicists* (Academic, San Diego, CA, 1995), 4th ed.

[20] G. V. Frisk, *Ocean and Seabed Acoustics: A Theory of Wave Propagation* (Prentice Hall, Englewood Cliffs, NJ, 1994).

[21] R. Snieder, "Extracting the Green's function from the correlation of coda waves: A derivation based on stationary phase," Phys. Rev. E **69**, 046610-1–8 (2004).

[22] R. Clayton and B. Engquist, "Absorbing boundary conditions for acoustic and elastic wave equations," Bull. Seismol. Soc. Am. **67**, 1529–1540 (1997).